

**Single versus double  $2p$  excitation in neon projectiles scattered from surfaces**D. Runco and P. Riccardi \**Dipartimento di Fisica Università della Calabria**and INFN—Gruppo Collegato di Cosenza, Via P. Bucci, 87036 Arcavacata di Rende, Cosenza, Italy* (Received 20 January 2021; revised 16 September 2021; accepted 28 September 2021; published 15 October 2021)

We scattered 0.45–5 keV  $\text{Ne}^+$  ions at Al surfaces, performing angle resolved measurements of electron spectra from autoionizing decay of excitations in the scattered projectiles, produced by electron promotion in close atomic encounters with target atoms. The shift and the broadening of the autoionization lines due to the motion of the emitting atoms in vacuum show that the double  $2p$  excitation in neon projectiles occurs simultaneously in a single scattering event and not in two consecutive collisions, as commonly assumed. Implications of our findings are commented upon for their relevance in research on charge exchange and energy deposition in ion-solid interactions, which are expected to be of interest for many fields.

DOI: [10.1103/PhysRevA.104.042810](https://doi.org/10.1103/PhysRevA.104.042810)**I. INTRODUCTION**

Charge exchange and electronic interactions during the scattering of charged particles at solid surfaces are important in a wide variety of research areas and applications, including spectroscopy and microscopy of surfaces and two-dimensional (2D) materials, gas discharge, particle accelerators, biomedical research, and the space environment [1–8]. Historically, the scattering of energetic ions at surfaces has been described by the classical dynamics of two-body elastic collisions. Within this framework, charge exchange phenomena have been included by the long range resonant, Auger, or plasmon assisted electron transfer processes [9–15], which occur at a large distance from the surface and therefore are treated separately from the close encounter of the projectile with a target atom. In real ion scattering events, however, there is clear evidence that inelastic effects during binary atomic collisions also play a crucial role in determining the charge and excitation states of the scattered projectiles [16–26]. For example, a substantial deviation from the prediction of the model of neutralization at a jellium surfaces has been recently reported for the ion fraction of sodium ions impinging on aluminum surfaces [16,17], and has been ascribed to the formation of extra  $\text{Na}^+$  ions due to the Auger decay of the projectiles' excited states [18], formed in collisions with Al atoms. These collisional excitations are generally described within a molecular orbital (MO) model, that describes the collision systems as transient quasimolecules in which some MOs are promoted to higher energies [27–29]. For atomic collisions in a solid environment, it is commonly accepted that excitation results from promotion of one electron into the continuum of conduction band states [30–32]. For the most investigated He and Ne projectiles, this process entails an inelastic loss of about 20 eV, due to the promotion of the projectiles'  $1s$  and  $2p$  levels, respectively [33,34].

Recently, this model has been used to interpret the large difference between the energy losses [24,25] of projectiles heavier than protons, including helium and neon, transmitted through Si foils along channeled and random trajectories, for which charge exchange collisions are more frequent. Since the energy loss of about 20 eV predicted in the one-electron excitation model is too low to account for the observed losses, it has been argued that electron capture and loss processes produce a trajectory dependence of the mean charge states, so that the collisionally reionized projectiles suffer larger energy losses while traveling along the random trajectory in a charged state, before being neutralized again by electron capture [25]. On the other hand, however, this interpretation neglects several known processes which entail larger energy losses, such as the simultaneous excitation of two  $2p$  electrons [35–47], and the involvement of a deeper electronic shell in the promotion process at higher impact energies [37,39,48–52].

In view of its relevance in both charge fractions and energy loss studies, in this work we address the question of the relative importance of one-electron versus simultaneous excitation of two  $2p$  electrons for neon projectiles at Al surfaces. We performed angle resolved measurements of electron spectra from autoionizing decay of  $2p$  excitations in the scattered projectiles, produced by electron promotion in close atomic encounters with target atoms. We discuss experimental evidence demonstrating that the excitation of two  $2p$  electrons in neon occurs simultaneously, in a single scattering event and not in two consecutive collisions, as expected in the one-electron excitation model.

**II. EXPERIMENTS**

The experiments were performed in a previously described UHV chamber setup [18,19], with a base pressure of  $3 \times 10^{-10}$  Torr. Singly charged neon ions were produced in an electron impact source, operated at a low discharge voltage of 30 V to avoid significant amounts of doubly charged ions

\*pierfrancesco.riccardi@unical.it

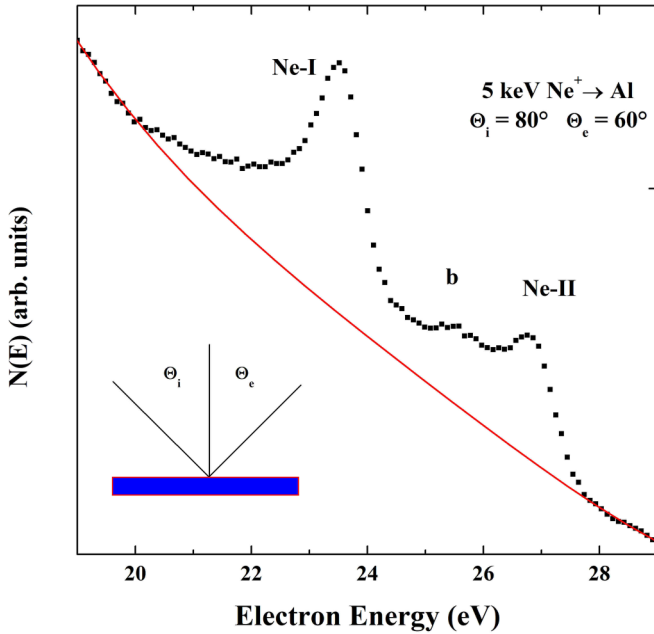


FIG. 1. Ne autoionization spectrum obtained by bombarding an Al surface with 5-keV  $\text{Ne}^+$  ions incident at an angle of  $\Theta_i = 80^\circ$  and an observation angle  $\Theta_e = 60^\circ$  relative to the surface normal.

reaching the surface with twice the energy. The absence of contamination with doubly charged ions was routinely verified by measuring the threshold energy for the observation of the Auger signal of both projectiles and target atoms [42]. The ion beam currents were of the order of  $10^{-9}$  A and had a Gaussian spatial distribution in both horizontal and vertical directions, as measured by a movable Faraday cup situated in the target position. To reduce the bombardment-induced topography problem and to avoid the change in the analyzer detection area with detection angles, the beam was set to raster over a large sample surface of  $4 \times 4 \text{ mm}^2$ , constant for all incidence angles. The polycrystalline Al samples (with 99.999% purity) were mounted on a rotatable manipulator and were sputter cleaned by 6-keV  $\text{Ar}^+$  bombardment. The energy distributions of emitted electrons were acquired by a hemispherical analyzer mounted on a rotatable goniometer that had semiacceptance angles of  $1.5^\circ$  and was operated at a constant pass energy of 20 eV. The incidence angle  $\Theta_i$  and the observation angle  $\Theta_e$  (measured with respect to the surface normal) were varied independently. The ion beam, the surface normal, and the analyzer axes were coplanar, as sketched in Fig. 1.

### III. FORMATION OF AUTOIONIZING STATES

Figure 1 reports a representative spectrum of electrons emitted with energies in the 18–30 eV energy range during the impact of  $\text{Ne}^+$  ions on an Al surface for an incident ion energy  $E_i = 5 \text{ keV}$  and for an incidence angle  $\Theta_i = 80^\circ$  and observation angle  $\Theta_e = 60^\circ$ . The spectrum shows two prominent features, labeled Ne-I and Ne-II in Fig. 1, and a weaker one labeled “b.” Ne-I and Ne-II are due, respectively, to the decay of a triplet  $\text{Ne}^{**}[2p^4(^3P)3s^2]$  and a singlet  $\text{Ne}^{**}[2p^4(^1D)3s^2]$  doubly excited state. As discussed below, the position and the

width of the peaks is typical of atomic transitions, indicating that they result from the decay in vacuum of reflected projectiles [35]. The formation of these excited states has been described within the framework of the “three steps” model, by dividing the interaction of the incoming ions with the surface into three segments: the incoming trajectory, the binary atomic collision, and the outgoing trajectory. In the first step, incoming ions are efficiently neutralized to their ground state [12,35,37], so that only a few percent survive as an ion. During the subsequent binary collision with an Al atom,  $2p$  excitation in neon occurs because of electron promotion. The promoted MO is the  $4f\sigma$  state, correlated to the  $2p$  atomic orbital of the lighter collision partner, as shown by correlation diagrams [17,27,28,35]. The final charge and excitation state of scattered projectiles is determined in the outgoing trajectory by charge exchange with the surface, that can alter the  $2p$  configuration and/or can feed their outer shell. This sequence of processes results in the formation of many  $2p$  excited states, whose decay produces several spectral features [35–41], the most prominent of which are Ne-I and Ne-II. An important aspect of these excitation processes in solids is that they result in the strong production of the triplet  $^3P$  state, which cannot be produced by the promotion of the  $4f\sigma$  state and is virtually absent in gas phase collisions [35]. This implies that the solid environment enables charge rearrangement mechanisms leading to the singlet to triplet conversion. Several possible charge rearrangement mechanisms have been proposed [35,37,40]. Here we observe that observation of the triplet state provides a first argument against the reionization model. Within the framework of the reionization mechanism [33], the triplet state can be created only in a collision involving a  $\text{Ne}^+$  that survived surface neutralization with a hole originally present in the  $2p$  level correlated to the  $3d\pi$  MO, so that the promotion of one  $4f\sigma$  electron leads to the triplet configuration. This implies that collisions involving neutral projectiles should not lead to the triplet configuration, in contrast with the very similar singlet to triplet intensity ratio observed for the impact of both  $\text{Ne}^+$  ions and  $\text{Ne}^0$  neutrals [35–38].

For the weak feature labeled “b” in Fig. 1, several initial excited states are possible [39]. These include  $\text{Ne}[2p^4(^3P)3s3p]$  of neutral Ne, the  $\text{Ne}^+[2p^3(^4S)3s^2(^4S)]$  and some  $\text{Ne}^+(2s2p^5nl)$  and  $\text{Ne}(2s2p^6nl)$  configurations. In particular, the  $\text{Ne}^+2p^3$  states can be formed in collisions involving  $\text{Ne}^+$  ions that have survived surface neutralization with a hole in the  $2p$  levels correlated with the  $3d\pi$  molecular orbital. The  $2s$  excitation becomes possible by  $3p\sigma-3p\pi$  rotational coupling closer to the united atom limit, which requires a small approach distance, consistently with the observation that the associated features become important at higher impact energies [39]. This last excitation has been revealed through photon spectroscopy for 15-keV  $\text{Ne}^+$  impact [37].

### IV. LINE-SHAPE VARIATIONS

The spectral features in Fig. 1 appear significantly shifted to higher energy, with respect to their expected values (20.35 eV for Ne-I and 23.55 eV for Ne-II). This is visualized in Fig. 2 which reports spectra acquired at varying incident ion energy in the range  $E_i = 0.45\text{--}5 \text{ keV}$  and for fixed incidence angle  $\Theta_i = 60^\circ$  and observation angle  $\Theta_e = 80^\circ$ . Since the

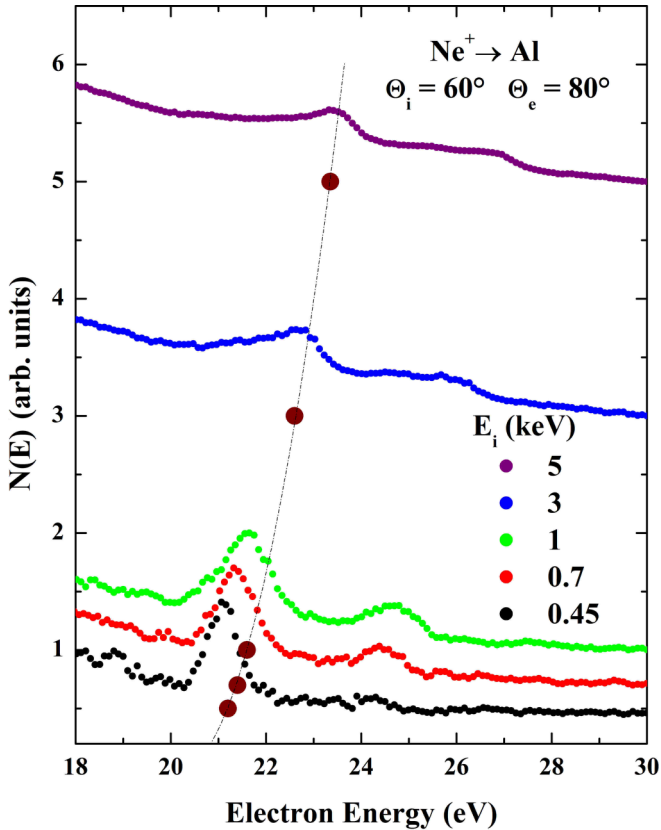


FIG. 2. Ne autoionization spectra at different energies for an incidence angle of  $\Theta_i = 60^\circ$  and an observation angle  $\Theta_e = 80^\circ$  relative to the surface normal. The spectra have been normalized to the same height, and shifted on the vertical scale in proportion to the ion energy. The circles mark the position of the Ne-I feature, showing a parabolic Doppler shift.

autoionizing projectiles are moving, the energy  $K_{\text{lab}}$  of Auger electrons measured in the laboratory frame will be shifted by  $\Delta K = K_{\text{lab}} - K_0 \sim mv_0v_I \cos \alpha = \sqrt{2mK_0}v_I \cos \alpha$ , where  $v_0 = \sqrt{\frac{2K_0}{m}}$  is the velocity of the electron in the frame of the projectile moving with velocity  $v_I$ , and  $\alpha$  is the angle between directions of motion of the atom and of the emitted electron (i.e.,  $v_I \cos \alpha$  is the component of the velocity of the emitting source in the analyzer direction);  $m$  is the electron mass, and we used the condition that  $v_I \ll v_0$ . The measured energy spectrum of emitted electrons is therefore “Doppler” shifted and broadened [53], according to the distribution of the velocity components of the decaying atoms in the direction of observation. The spectra in Fig. 2 are shifted vertically by an amount proportional to the energy of incoming projectiles, which aids the visualization of the Doppler shift caused by the motion of the autoionizing scattered particle, as it is indicated by the parabolic line indicating the position of the peak Ne-I [41,42]. At low impact energies scattered projectiles have low energy and the peaks appear quite symmetric, and their position is close to the unshifted value. With increasing incident energy, scattered projectiles have higher energy, so that the electrons collected in a forward direction will be revealed with a positive energy shift, since the scattered flux is on average traveling toward the analyzer.

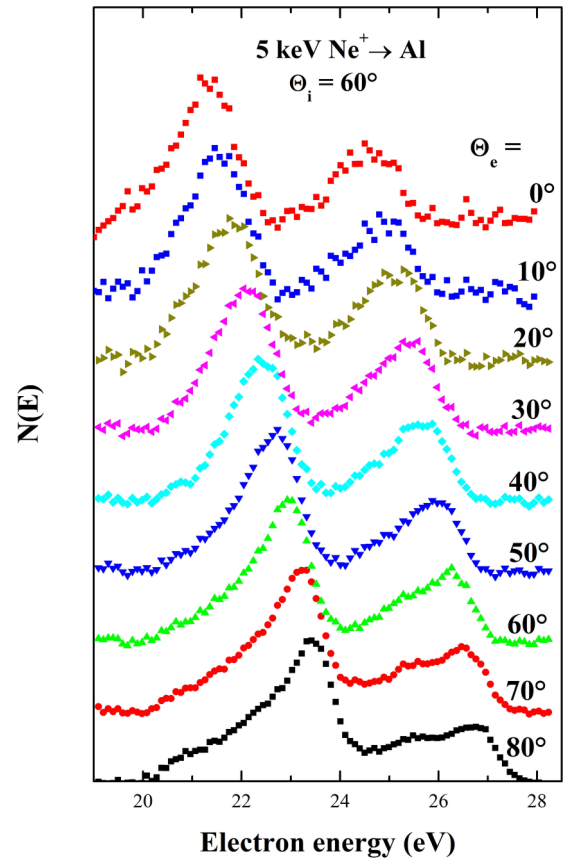


FIG. 3. Detection-angle-resolved Ne autoionization spectra for a primary energy of  $E_i = 5\text{-keV}$  for an incidence angle of  $\Theta_i = 60^\circ$  relative to the surface normal. The spectra have been background subtracted, normalized to the same height, and arbitrarily shifted on the vertical scale.

With increasing ion energy, the spectra become also increasingly asymmetric, broadening on the low energy side, due to electrons emitted by excited neon atoms scattered with lower components of velocity in the observation direction. These projectiles with low components of velocity in the observation directions reveal the contribution to the emission of projectiles severely scattered, such as those excited in sub-surface collisions. To gain more insight into the line-shape changes of the spectral features, we performed measurements as a function of the observation and the incidence angles.

Figure 3 reports the background subtracted spectra of electrons emitted by the impact of 5-keV  $\text{Ne}^+$  ions on Al for an incidence angle  $\Theta_i = 60^\circ$  at varying observation angles  $\Theta_e$ . The spectra have been normalized to the same maximum height to compare line shapes. Figure 3 shows that the peak energy increases as  $\Theta_e$  is changed from  $0^\circ$  to  $80^\circ$ . The shift toward higher energies of the peaks in Fig. 3 reveals that components of velocity in the direction of observation of the emitting neon are on average increasing with  $\Theta_e$ . Since the classical physics of two-body collisions shows that the energy of the scattered projectile increases as the scattering angle is decreased, this observation is a clear signal of the dominance of the single scattering regime, consistently also with results of simulations reported in the literature [37,38].

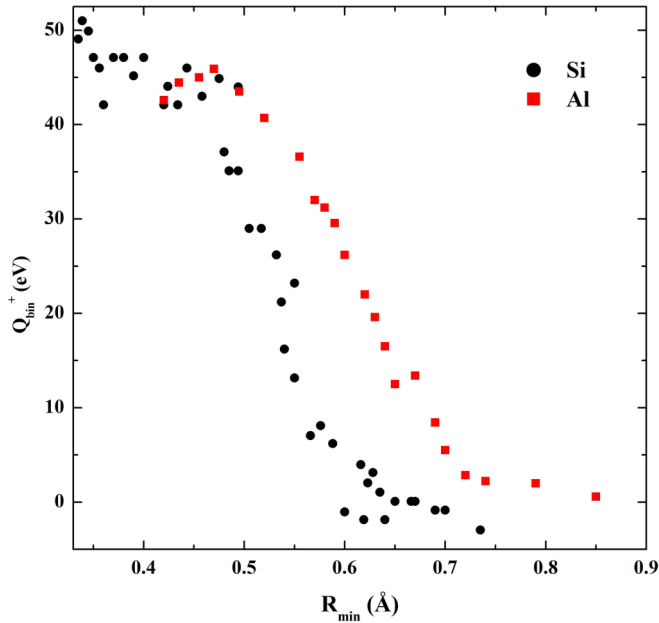


FIG. 4. Hard collision inelasticities for scattered  $\text{Ne}^+$  resulting from  $\text{Ne}^+$  impact on Al [44] and on Si [43].

This conclusion is further corroborated by comparison with the inelasticities  $Q_{\text{bin}}$  (reproduced in Fig. 4 from Refs. [43,44]) measured in single scattering experiments of Ne ions on Al and Si as a function of the closest approach distance  $R_{\text{min}}$ . Starting from a threshold of about 0.7–0.8 Å,  $Q_{\text{bin}}$  for Al steadily increase as  $R_{\text{min}}$  decreases until saturation behavior occurs for both targets for  $R_{\text{min}}$  around 0.5 Å. Collisions with Si targets show the same behavior with a lower  $R_{\text{min}}$ , due to the larger mass of the target atom. For both targets, the values of  $Q_{\text{bin}}$  in the saturation region correspond to the 45-eV loss needed to form the doubly excited autoionizing states of Ne in the hard collision from a projectile that has been neutralized on the incoming path. Evidence for direct ionization of  $\text{Ne}^0$  to  $\text{Ne}^+$  ( $Q_{\text{bin}} \sim 20$  eV), expected in the one-electron excitation and reionization model, has not been observed. Therefore, there is full correspondence between energy losses measured in ion scattering experiments and electron spectroscopy data relating to the autoionizing decay of neon projectiles, which verifies that the simultaneous excitation of the two  $2p$  electrons in neon projectiles is conclusively established.

As mentioned above, Figs. 1–3 also reveal the onset of a low energy tailing which asymmetrically broadens the spectra. This broadening is therefore due to electrons emitted by projectiles scattered with lower components of velocity in the observation directions. The low energy tail extends down to the value of the unshifted peaks, indicating that the majority of the decaying atoms are moving with velocity components toward the analyzer. To investigate the origin of these projectiles scattered with low components of velocity in the observation directions we performed measurements at varying the incidence angle of the neon beam. Figure 5 reports the variation of the spectral line shape with the incidence angle  $\Theta_i$  for fixed ion energy  $E_i = 5$  keV and observation angle  $\Theta_e = 60^\circ$ . The spectra are reported normalized to beam current and width. At near normal incidence, the autoionization peaks in Fig. 5

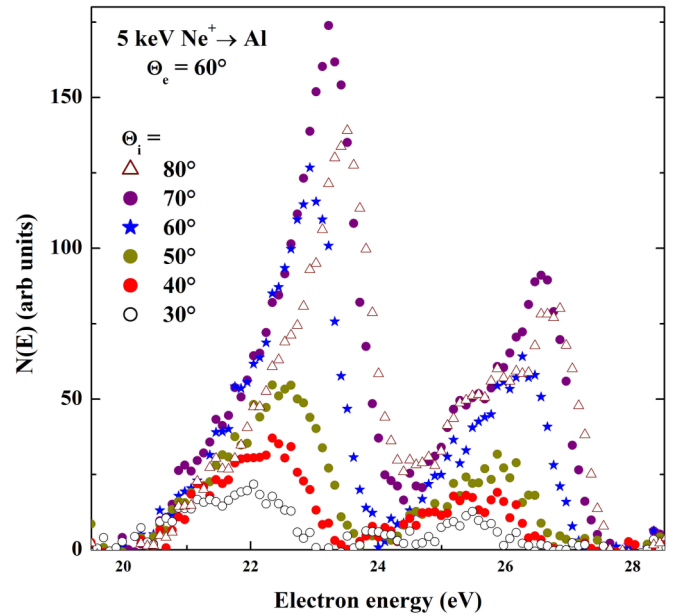


FIG. 5. Background subtracted autoionization spectra of neon at varying the incidence angle  $\Theta_i$ , for a primary energy of  $E_i = 5$  keV and an observation angle of  $\Theta_e = 60^\circ$  relative to the surface normal. The spectra have been normalized to the beam current and width.

are very weak because most of the projectiles penetrate inside the solid. Moreover, the peaks appear close to the unshifted value because electrons are emitted by slow projectiles that have been reflected in vacuum after being severely deflected in a large angle scattering event or in a sequence of collisions inside the solid. As the ion beam is moved to oblique incidence, the Auger intensity increases and the Doppler effects in the position and the asymmetrically broadened line shapes appear because single scattering events produce with increasing efficiency energetic excited projectiles reflected in vacuum. Our conclusions agree with earlier experimental results for the Ne-Al and the Ne-Mg collision systems at lower energies [37,41]. These experiments showed that the intensity of the autoionization lines Ne-I and Ne-II increase and reach maximum values around  $70^\circ$ – $80^\circ$ . At larger incidence angle the intensity of emission decreases because the projectiles cannot get close enough to the target atom to determine excitation, as also shown by simulations [37]. This is also consistent with the strong suppression of the autoionization peaks at grazing incidence on carefully prepared flat surfaces [39].

## V. CONCLUDING REMARKS

Thus the shift and the asymmetric broadening of the autoionization peaks are determined by the angular and energy distributions of excited scattered projectiles, reflecting the kinematic properties of two-body scattering. This allows us to conclude that double excitations in reflected projectiles are efficiently produced in single scattering events. When this scattering event occurs inside the solid during the collision cascade, prevalent for near normal incidence, the excited projectiles will be reflected with low energy and revealed in the asymmetric spectral broadening.

The above results have implications in recent investigations on energy deposition [24,25] and on charge fraction measurements [16,17]. For instance, the energy losses of heavy ions transmitted through Si foils along random trajectories [24,25] can be traced back to the several promotion processes that are operative in the energy range from several tens to some hundreds of keV of those experiments. Besides the  $4f\sigma$  and the  $3p\sigma$ - $3p\pi$  promotion discussed above, also the  $2p\sigma$ - $2p\pi$  promotion [48,49] should be considered. For collisions in solid targets, promotion from the  $2p\sigma$  MO (correlated to the  $1s$  level of the lighter atom) is possible, provided charge transfer and/or solid target effects in previous collisions produced holes in the  $L_{2,3}$  levels of the heavier partner, correlated to the  $2p\pi$  MO [48].  $K$  x-ray emission from Si and Ne has been identified for the Ar-Si system [50] and from neon impacting on Mg, Al, and Si [51,52]. These observations imply large energy losses per collision. For example, the  $K$  line of Si is at  $\sim 1740$  eV. A few of these processes explain the different energy losses of Ar and Si projectiles along random and channeled trajectories (see Fig. 2 of Ref. [24]). Similar x-ray emission should be observed also in the experiments under consideration.

The autoionization emission provides direct evidence that ion production at the Al surface is determined by collisional electronic excitation, as recently reported for sodium projectiles, which show similar electron promotion effects to those here reported for neon [16–19]. These electron promotion effects depend on the actual charge states of the projectiles at the moment of collision, that for neon leads to the production of both  $2p$  doubly and triply excited states. The decay of these excited states results, respectively, in the production of singly and doubly charged ions that determine the scattered ion fractions. The same conclusion holds for sodium projectiles, since the parent autoionizing states of sodium have been identified in electron spectroscopy experiments [18].

In summary, the simultaneous excitation of two  $2p$  electrons in neon projectiles colliding with Al target atoms and its dominance over one-electron excitation is undisputed. We expect that a sizable fraction of doubly charged ions should be observed also in the case of sodium projectiles. Since several promotion processes become operative with increasing energies, the trajectory dependence of the energy losses recently reported in Si samples needs to be reexamined, properly considering collisional excitations that entail deep shell promotion and large energy losses.

- 
- [1] P. Sigmund, *Particle Penetration and Radiation Effects*, Springer Series in Solid-State Sciences Vol. 151 (Springer, Berlin, 2006).
- [2] P. Sigmund, *Particle Penetration and Radiation Effects. Volume 2*, Springer Series in Solid-State Sciences Vol. 179 (Springer, Berlin, 2014).
- [3] R. A. Baragiola and P. Riccardi, in *Reactive Sputter Deposition*, edited by D. Depla and S. Mahieu, Springer Series in Materials Science Vol. 109 (Springer, Berlin, 2008), Chap. 2.
- [4] A. Sindona, M. Pisarra, M. Gravina, C. Vacacela Gomez, P. Riccardi, G. Falcone, and F. Plastina, *Beilstein J. Nanotechnol.* **6**, 755 (2015).
- [5] H. H. Brongersma, M. Draxler, M. de Ridder, and P. Bauer, *Surf. Sci. Rep.* **62**, 63 (2007).
- [6] A. Sindona, M. Pisarra, C. V. Gomez, P. Riccardi, G. Falcone, and S. Bellucci, *Phys. Rev. B* **96**, 201408(R) (2017).
- [7] L. Scipioni, L. A. Stern, J. Notte, S. Sijbrandij, and B. Griffin, *Adv. Mater. Process.* **166**, 27 (2008).
- [8] J. L. Fox, M. I. Galand, and R. E. Johnson, *Space Sci. Rev.* **139**, 3 (2008).
- [9] H. D. Hagstrum, *Phys. Rev.* **150**, 495 (1966).
- [10] R. C. Monreal, *Prog. Surf. Sci.* **89**, 80 (2014).
- [11] R. A. Baragiola and C. A. Dukes, *Phys. Rev. Lett.* **76**, 2547 (1996).
- [12] M. Beckschulte and E. Taglauer, *Nucl. Instrum. Methods Phys. Res., Sect. B* **78**, 29 (1993).
- [13] A. Sindona, P. Riccardi, S. Maletta, M. Pisarra, and A. Cupolillo, *Vacuum* **84**, 1038 (2010).
- [14] A. Sindona, M. Pisarra, P. Riccardi, and G. Falcone, *Nanosci. Nanotechnol. Lett.* **4**, 1050 (2012).
- [15] N. Lorente and R. Monreal, *Surf. Sci.* **303**, 253 (1994).
- [16] P. Liu *et al.*, *Phys. Rev. A* **101**, 032706 (2020).
- [17] M. Wei *et al.*, *Nucl. Instrum. Methods Phys. Res., Sect. B* **478**, 239 (2020).
- [18] P. Riccardi, F. Cosimo, and A. Sindona, *Phys. Rev. A* **97**, 032703 (2018).
- [19] N. Ligato, A. Cupolillo, A. Sindona, P. Riccardi, M. Pisarra, and L. S. Caputi, *Surf. Sci.* **626**, 40 (2014).
- [20] R. Souda and M. Aono, *Nucl. Instrum. Methods Phys. Res., Sect. B* **15**, 114 (1986).
- [21] R. Souda, T. Aizawa, C. Oshima, S. Otani, and Y. Ishizawa, *Surf. Sci.* **194**, L119 (1988).
- [22] M. A. Sortica, V. Paneta, B. Bruckner, S. Lohmann, M. Hans, T. Nyberg, P. Bauer, and D. Primetzhofer, *Phys. Rev. A* **96**, 032703 (2017).
- [23] P. Riccardi, A. Sindona, and C. A. Dukes, *Nucl. Instrum. Methods Phys. Res., Sect. B* **382**, 7 (2016).
- [24] S. Lohmann, R. Holeňák, and D. Primetzhofer, *Phys. Rev. A* **102**, 062803 (2020).
- [25] S. Lohmann and D. Primetzhofer, *Phys. Rev. Lett.* **124**, 096601 (2020).
- [26] P. Riccardi, R. A. Baragiola, and C. A. Dukes, *Phys. Rev. B* **92**, 045425 (2015).
- [27] U. Fano and W. Lichten, *Phys. Rev. Lett.* **14**, 627 (1965).
- [28] M. Barat and W. Lichten, *Phys. Rev. A* **6**, 211 (1972).
- [29] P. Riccardi, A. Sindona, and C. A. Dukes, *Phys. Rev. A* **93**, 042710 (2016).
- [30] R. Souda, T. Aizawa, C. Oshima, and Y. Ishizawa, *Nucl. Instrum. Methods Phys. Res., Sect. B* **45**, 364 (1990).
- [31] S. Tsuneyuki and M. Tsukada, *Phys. Rev. B* **34**, 5758 (1986).
- [32] Y. Muda and D. M. Newns, *Phys. Rev. B* **37**, 7048 (1988).
- [33] R. Souda, K. Yamamoto, W. Hayami, T. Aizawa, and Y. Ishizawa, *Phys. Rev. Lett.* **75**, 3552 (1995).
- [34] R. Souda, K. Yamamoto, W. Hayami, T. Aizawa, and U. Ishizawa, *Surf. Sci.* **363**, 139 (1996).
- [35] G. Zampieri, F. Meier, and R. Baragiola, *Phys. Rev. A* **29**, 116 (1984).

- [36] O. Grizzi, M. Shi, H. Bu, J. W. Rabalais, and R. A. Baragiola, *Phys. Rev. B* **41**, 4789 (1990).
- [37] L. Guillemot, S. Lacombe, M. Maazouz, V. N. Tuan, V. A. Esaulov, E. A. Sanchez, Y. Bandurin, A. Daschenko, and V. Droblich, *Surf. Sci.* **365**, 353 (1996).
- [38] V. A. Esaulov, L. Guillemot, and S. Lacombe, *Nucl. Instrum. Methods, Phys. Res., Sect. B* **90**, 305 (1994).
- [39] O. Grizzi, E. A. Sánchez, J. E. Gayone, L. Guillemot, V. A. Esaulov, and R. A. Baragiola, *Surf. Sci.* **469**, 71 (2000).
- [40] F. Xu, R. A. Baragiola, A. Bonanno, P. Zoccali, M. Camarca, and A. Oliva, *Phys. Rev. Lett.* **72**, 4041 (1994).
- [41] F. Xu, N. Mandarino, A. Oliva, P. Zoccali, M. Camarca, A. Bonanno and R. A. Baragiola, *Phys. Rev. A* **50**, 4040 (1994).
- [42] P. Riccardi, A. Sindona, and C. A. Dukes, *Phys. Lett. A* **381**, 1174 (2017).
- [43] F. Xu, G. Manicò, F. Ascione, A. Bonanno, A. Oliva, and R. A. Baragiola, *Phys. Rev. A* **57**, 1096 (1998).
- [44] M. J. Gordon, J. Mace, and K. P. Giapis, *Phys. Rev. A* **72**, 012904 (2005).
- [45] J. Mace, M. J. Gordon, and K. P. Giapis, *Phys. Rev. Lett.* **97**, 257603 (2006).
- [46] H. Eder, F. Aumayr, P. Berlinger, H. Störi, and H. P. Winter, *Surf. Sci.* **472**, 195 (2001).
- [47] G. Manicò, F. Ascione, N. Mandarino, A. Bonanno, P. Riccardi, P. Alfano, P. Zoccali, A. Oliva, M. Camarca, and F. Xu, *Surf. Sci.* **392**, L7 (1997).
- [48] U. Wille and R. Hippler, *Phys. Rep.* **132**, 129 (1986).
- [49] Y. Guo, Z. Yang, B. Hu, X. Wang, Z. Song, Q. Xu, B. Zhang, J. Chen, B. Yang, and J. Yang, *Sci. Rep.* **6**, 30644 (2016).
- [50] J. Macek, J. A. Cairns, and J. S. Briggs, *Phys. Rev. Lett.* **28**, 1298 (1972).
- [51] K. Taulbjerg, B. Fastrup, and E. Laegsgaard, *Phys. Rev. A* **8**, 1814 (1973).
- [52] C. Foster, T. Hoogkamer, and F. Saris, *J. Phys. B: Atom. Mol. Phys.* **7**, 2563 (1974).
- [53] A. Bonanno, F. Xu, M. Camarca, R. Siciliano, and A. Oliva, *Phys. Rev. B* **41**, 12590 (1990).